

# Properties of novel bone hemostat prepared using hydroxyapatite, phosphoryl oligosaccharides of calcium and thermoplastic resin

Tokio MIMURA, Tomohiro UMEDA, Yoshiro MUSA\* and Kiyoshi ITATANI†

Department of Materials and Life Sciences, Faculty of Science and Engineering, Sophia University,  
7-1 Kioi-cho, Chiyoda-ku, Tokyo 102-8554, Japan

\*2nd Department of Orthopaedic Surgery, School of Medicine, Toho University,  
2-17-6 Ohashi, Meguro-ku, Tokyo 153-8515, Japan

A novel hemostatic agent was prepared using phosphoryl oligosaccharides of calcium (POs-Ca), hydroxyapatite [ $\text{Ca}_{10}(\text{PO}_4)_6(\text{OH})_2$ ; HAp] obtained by the hydrolysis of POs-Ca (i.e., sugar-containing HAp (*s*-HAp), Ca/P ratio = 1.56, 60.3 mass% calcium-deficient HAp and 39.5 mass% organic materials) and thermoplastic resin (random copolymer of ethylene oxide and propylene oxide; EPO). The gel formed by mixing the EPO with water (EPO/water mass ratio: 0.20) was flash frozen at  $-80^\circ\text{C}$  and then freeze-dried at  $-50^\circ\text{C}$  for 15 h. The freeze-dried material was blended with POs-Ca or *s*-HAp. The hemostat, whose consistency had been adjusted to that of commercial hemostat by adding water, possessed the stanching times: 6.0 h (*s*-HAp/EPO hemostat; *s*-HAp/EPO = 0.20) > 5.75 h (POs-Ca/EPO hemostat; POs-Ca/EPO = 0.20) > 4.75 h (EPO hemostat). The test for the implantation of these composite hemostats into the Japanese white rabbits indicated that the bone regeneration of *s*-HAp/EPO composite hemostat was excellent, compared to the case of POs-Ca/EPO composite hemostat. The loading of gentamicin, a typical antibiotic agent, to the *s*-HAp/EPO composite hemostat showed the steady state releasing in the phosphate buffered saline.

©2013 The Ceramic Society of Japan. All rights reserved.

Key-words : Bone hemostat, Hydroxyapatite, Phosphoryl oligosaccharides of calcium, Thermoplastic resin, Drug releasing properties

[Received July 12, 2012; Accepted October 29, 2012]

## 1. Introduction

When bones are cut open during a surgery, a large amount of bleeding occurs from the bone's vessel. There are three techniques to stop bleeding, (i) thermal hemostasis, (ii) mechanical hemostasis, and (iii) chemical hemostasis.<sup>1)</sup> Most useful hemostat is a bone wax, whose major component is beewax, which may stop bleeding by the mechanical hemostasis. Unfortunately, the hemostats practically used are not fully biocompatible and sometimes cause infection, because it is derived from animals.<sup>2)</sup> On the other hand, a block copolymer of "ethylene oxide and propylene oxide" is now commercially available for filling the bone defects.<sup>3),4)</sup> The problem of it may be that the poor flexibility makes its utilization as a hemostat difficult. Taking into account the utilization of EPO for hemostat, the random copolymer of EPO must be favorable rather than the block form, because it has excellent flexibility and adhesion performances. The random copolymer of EPO (hereafter describes only as EPO) with excellent flexibility and adhesion, as well as the biocompatibility and infection prevention, are expected to be available as a novel hemostat.

The phosphoryl oligosaccharides of calcium (POs-Ca), which is available for edulcorant, is extracted from the potato starch.<sup>5),6)</sup> The advantages of POs-Ca may be that it has groups of  $\text{Ca}^{2+}$  and  $\text{PO}_4^{3-}$ , which is the potential ability of re-calcification, and that it is easily dissolved in water; the maximum amount of POs-Ca dissolved in water is estimated to be 50 mass%. By making use of such advantages, the present authors<sup>7)</sup> have prepared a

sugar-containing hydroxyapatite [ $\text{Ca}_{10}(\text{PO}_4)_6(\text{OH})_2$ ; *s*-HAp] from POs-Ca solution through the hydrothermal treatment. Thus the POs-Ca, as well as its hydrolyzed materials (*s*-HAp, i.e., HAp and organic components), may be available as biomaterials.

As shown above, the ideas of designing novel hemostatic agents are based upon the flexibility, adhesion, biocompatibility and infection prevention, as well as the stanching effect. Taking these performances into account, the authors paid attention to the development of a novel hemostat through the combination of POs-Ca, *s*-HAp and thermoplastic resin (EPO), as shown in Fig. 1. On the basis of such background, the present paper describes the optimized preparation conditions of novel materials for stanching the blood, using POs-Ca, *s*-HAp and EPO.

## 2. Materials and methods

The starting materials used for the designing of hemostat were POs-Ca and EPO. The commercial POs-Ca was hydrolyzed by hydrothermally treating 10 mass% POs-Ca solution at a temperature between 100 and  $110^\circ\text{C}$  for 5 h. On the other hand, the commercial EPO was mixed with de-ionized water to form gel (mass ratio of EPO to water: 1.0) and allowed to stand for 1 to 2 d. This mixture was frozen at  $-80^\circ\text{C}$  and then dried at  $-50^\circ\text{C}$  for 9 to 20 h. The freeze-dried mixture was ground by using a mechanical mixer. The ground powder was sieved into three grain-size fractions, (i) 0.5–1.0 mm, (ii) 1.0–2.0 mm and (iii) over 2.0 mm.

In order to check the operation performance of gel, the consistency was examined measuring the spread size, after the gel was set between two plates and loaded with a mass of 500 g. The stanching of blood was evaluated by checking the time that the paper on the hemostat started to be wet by the simulated

† Corresponding author: Dr. K. Itatani; E-mail: itatani@sophia.ac.jp

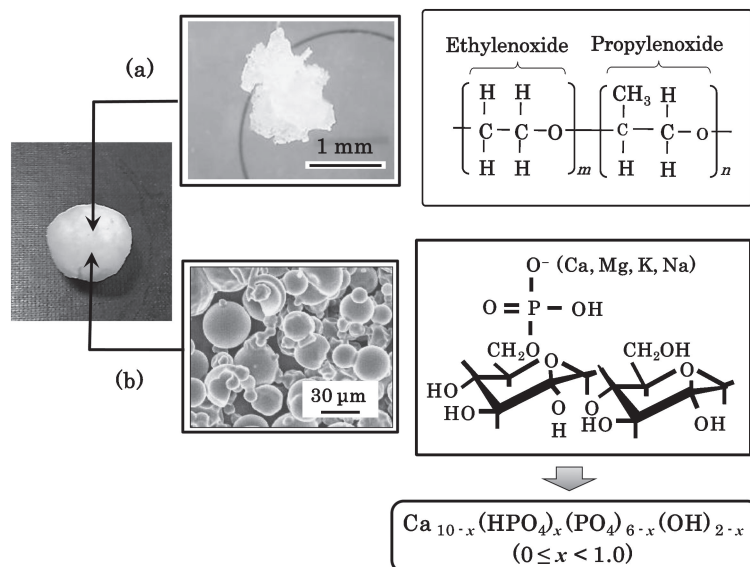


Fig. 1. Schematic diagram of overall view, (a) EPO (optical micrograph) and (b) POs-Ca (FE-SEM micrograph).

blood come out the top of a porous HAp cube (porosity of 70% and mean pore size of 200 μm), due to the capillary force.<sup>8)</sup>

The phase identification was carried out using an X-ray diffractometer (XRD; RINT 2000V/P, Rigaku Corp., Tokyo, 40 kV and 40 mA) with monochromatic Cu Kα radiation and a Fourier transform infra-red spectrometer (FT-IR; 8600PC, Shimadzu, Kyoto). Phase changes during the heating from room temperature to 1200°C were examined by differential thermal analysis and thermogravimetry (DTA-TG; Model Thermo Plus TG8120, Rigaku, Tokyo). The specific surface area of the powder was measured by the BET method, using nitrogen (N<sub>2</sub>) as the adsorption gas. The observation of the particles was conducted using a field-emission scanning electron microscope (FE-SEM: Model SU-8000, Hitachi, Tokyo) with an accelerating voltage of 5 kV or a transmission electron microscope (TEM: Model JEM-2011, JEOL, Tokyo; accelerating voltage, 200 kV). The chemical composition of the powder was examined using an energy dispersive electron X-ray microanalyzer (EDX; EX-210, Horiba, Kyoto), attached to the FE-SEM.

The composite hemostats were implanted in the femur and tibia of Japanese white rabbits for 4 or 9 weeks. The degree of bone regeneration was observed on the basis of the non-decalcified specimens prepared with a Villanueva bone stain, using an inverted microscope (Axiovert135, Carl Zeiss Japan, Tokyo). The releasing amount of gentamicin was evaluated by *o*-phthalaldehyde method.<sup>9)</sup> Firstly, gentamicin sulfate (10 mg) was mixed with the gel (1 g). After the gentamicin-containing gel was immersed in the 10 cm<sup>3</sup> phosphate buffered saline [PBS(-)] at 37.0°C for 10 h, the releasing behavior of gentamicin from the gel was examined by measuring the absorbance of the sample solution containing 2-propanol at 332.0 nm by using a spectrophotometer (BioSpec-1600, Shimadzu, Kyoto). In this experiment, PBS(-) solution was replaced with new one at each sampling.<sup>10),11)</sup>

### 3. Results and discussion

#### 3.1 Preparation of HAp from the hydrothermally-treated POs-Ca

In order to prepare the HAp powder from POs-Ca, the hydrothermal treatment was conducted at a temperature between 100

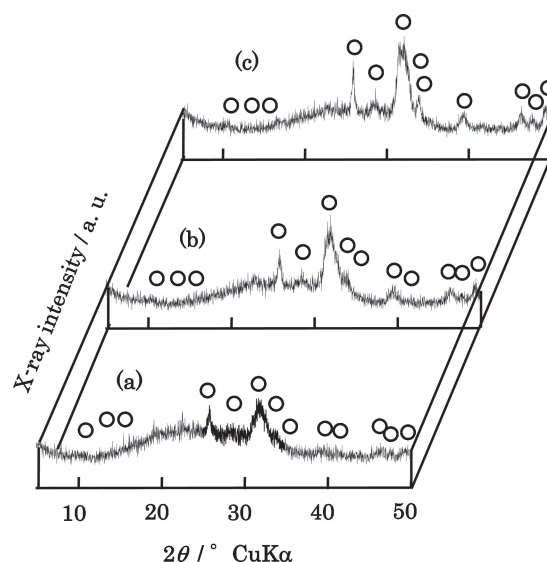


Fig. 2. XRD patterns of the powders formed by the hydrothermal treatment of 10 mass% POs-Ca aqueous solution at (a) 100°C for 5 h, (b) 105°C for 5 h and (c) 110°C for 5 h. ○: HAp.

and 110°C for 5 h. When the POs-Ca solution was hydrothermally treated at 105 and 110°C for 5 h, the precipitation occurred to form the powder. Although no precipitation occurred at the hydrothermal temperature of 100°C, the precipitates were instantaneously obtained by the addition of ethanol to the solution after cooling to room temperature.

Figure 2 shows typical XRD patterns of hydrothermally treated powders at a temperature between 100 and 110°C for 5 h. XRD patterns of the hydrothermally-treated powders showed the presence of poorly crystallized HAp.<sup>12)</sup>

The amounts of Ca and P of hydrothermally-treated powders were measured using an EDX. The molar ratio of Ca to P of the powder hydrothermally-treated at 100°C for 5 h was calculated to be 1.56. On the other hand, Ca/P ratios of the powders hydrothermally-treated at 105 and 110°C were 1.53 and 1.51, respec-

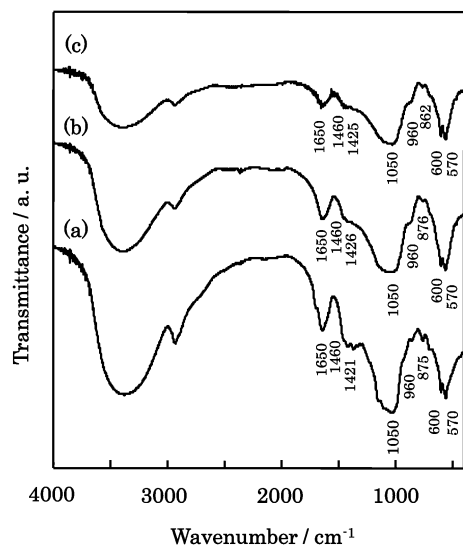


Fig. 3. FT-IR spectra of precipitates formed by the hydrothermal reaction of 10 mass% POs-Ca aqueous solution at (a) 100°C for 5 h, (b) 105°C for 5 h and (c) 110°C for 5 h.

tively. These analytical results indicate that the hydrothermally-treated powders were composed of calcium-deficient HAp with the general formula of  $\text{Ca}_{10-x}(\text{HPO}_4)_x(\text{PO}_4)_{6-x}(\text{OH})_{2-x} \cdot n\text{H}_2\text{O}$  ( $0 \leq x < 1.0$ ). Since the Ca/P ratio of powder hydrothermally-treated at 100°C for 5 h was 1.56, the calcium-deficient HAp, for example, can be expressed as  $\text{Ca}_{9.36}(\text{HPO}_4)_{0.64}(\text{PO}_4)_{5.36}(\text{OH})_{1.36} \cdot n\text{H}_2\text{O}$  ( $x = 0.64$ ).

As the XRD patterns indicate, the presence of poorly-crystalline HAp suggests that the amorphous materials or organic materials must be present in the hydrothermally-treated powders.

**Figure 3** shows the FT-IR spectra showing the phases present in the hydrothermally-treated powders. FT-IR spectra of the powders hydrothermally treated at 100–110°C for 5 h showed absorption peaks at around 570, 600, 870, 960, 1050, 1425, 1460 (shoulder) and 1650  $\text{cm}^{-1}$ , together with the broad absorption band in the range of 3200 to 3700  $\text{cm}^{-1}$ .

The absorption peaks at 570, 600, 960 and 1050  $\text{cm}^{-1}$  are assigned to the  $\text{PO}_4^{3-}$  in the HAp structure. The absorption peak at 1650  $\text{cm}^{-1}$  and the absorption band in the range of 3200 to 3700  $\text{cm}^{-1}$  are assigned to the physically-adsorbed water and the hydroxyl group in the HAp and POs-Ca.<sup>(13)</sup> Relating to the presence site of  $\text{CO}_3^{2-}$  in HAp structure, the characteristic absorption peaks at 880, 1450 and 1545  $\text{cm}^{-1}$  may be regarded as the substitution site of “Type A”, i.e., substitution of  $\text{CO}_3^{2-}$  for  $\text{OH}^-$  site in HAp, whereas the absorption peaks at 870, 1410–1420 and 1460–1470  $\text{cm}^{-1}$  are regarded as the substitution site of “Type B”, i.e., substitution of  $\text{CO}_3^{2-}$  for  $\text{PO}_4^{3-}$  site in HAp. Further, the substitution of  $\text{CO}_3^{2-}$  for both  $\text{OH}^-$  and  $\text{PO}_4^{3-}$  sites is regarded as “Type AB”, whose absorption peaks appeared in the ranges of 850–890  $\text{cm}^{-1}$  and 1400–1650  $\text{cm}^{-1}$ . Based upon the present data, we considered that the carbonate ions are partly substituted for the site of OH in HAp structure, i.e., Type B.<sup>(14)</sup>

**Figure 4** shows the changes in specific surface area of the powder with hydrothermal temperature, together with typical TEM micrographs. The specific surface area of the powder exponentially increased from 4.0 to 42.2  $\text{m}^2 \cdot \text{g}^{-1}$  with increasing temperature from 100 to 110°C for 5 h. TEM micrograph of the powder hydrothermally-treated at 100°C for 5 h showed that the small particles with sizes of approximately 20 nm were stuck

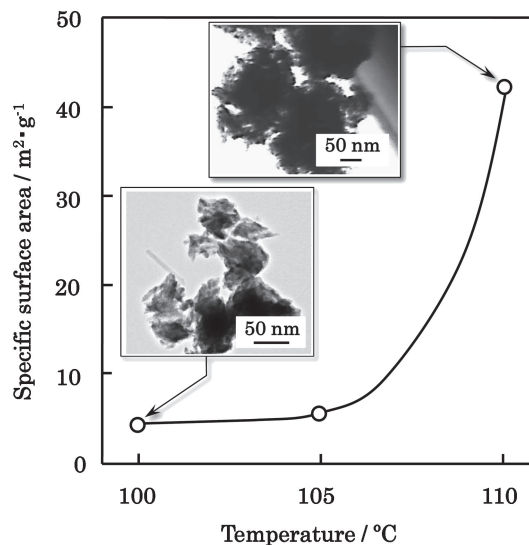


Fig. 4. Changes in specific surface area of precipitant with increasing hydrothermal temperature (hydrothermal time: 5 h at each temperature), together with TEM micrographs.

together to form aggregates. On the other hand, TEM micrograph of the powder hydrothermally-treated at 110°C for 5 h showed that the small particles with sizes of approximately 2 nm were stuck together to form aggregates.

Compared to the particle sizes of the powders hydrothermally-treated at 100 and 110°C for 5 h, the former particles sizes appeared to be larger than the latter particle sizes. This phenomenon is not so surprising, since the particle size of HAp was larger with increasing temperature. The larger particle size of the powder hydrothermally-treated at 100°C for 5 h may be achieved by the adhesion of small HAp particles, due to the presence of POs-Ca derived organic compound.

The results obtained so far indicate that the hydrothermally-treated powers may contain not only calcium-deficient HAp but organic components. In addition to the phase identification conducted by XRD and FT-IR, the presence and amount of organic components were examined using the DTA-TG and XRD. The results are shown in **Fig. 5**. On the basis of DTA results of the powder hydrothermally-heated at 100°C for 5 h, the broad exothermic events occurred over the range of 200 to 550°C [solid line in Fig. 5(a)]. On the other hand, DTA curve of POs-Ca contained the broad exothermic events in the range of 200 to 450°C and 450 to 700°C [dotted line in Fig. 5(a)]. On the basis of the phase changes examined by XRD, X-ray intensity of HAp started to be reduced above 500°C and became almost zero at 700°C, whereas  $\beta$ -TCP,<sup>(15)</sup> which appeared at 500°C, increased with temperature [Fig. 5(b)]. Further, TG results showed that the step-wise mass losses occurred in the ranges of 200 to 500°C and 500 to 800°C [Fig. 5(c)].

According to the DTA-TG and XRD results, the phase changes during the heating of *s*-HAp may be occurred by the routes of (1) the formation of carbon through the thermal decomposition of *s*-HAp [(i); 200–500°C], (2) the release of CO due to the oxidation of residual carbon [(ii); 500–800°C] and (3) the formation of  $\beta$ -TCP (>500°C). Based upon the TG results, the amount of mass loss, 39.5 mass% [(iii); (i) + (ii)], indicates the presence of organic components and 60.3 mass% of HAp [(iv)]. The molecular structures of organic components in the *s*-HAp seem to be a little different from that of POs-Ca but essentially preserve the basic units of POs-Ca structure, because the exothermic events of

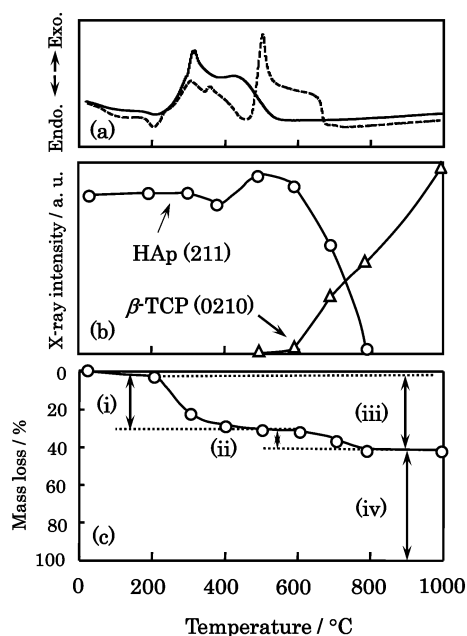


Fig. 5. (a) DTA curve, (b) phase changes (determined by XRD) and (c) changes in mass loss with increasing temperature. Note that the dotted line indicates the DTA curve of pure POs-Ca. Heating rate:  $10^{\circ}\text{C}\cdot\text{min}^{-1}$ .

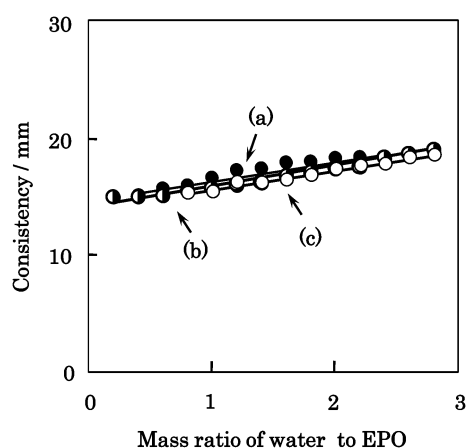


Fig. 6. Changes in consistency of EPO hemostat with increasing amount of water. Grain size of EPO: (a) 0.5–1.0 mm (b) 1.0–2.0 mm (c)  $>2.0$  mm.

hydrothermally-treated powder were shifted toward the lower temperature, compared to the case of POs-Ca powder.

### 3.2 Optimization for the fabrication conditions of hemostat

The consistency of the commercial hemostat measured in this research was 18.2 mm. **Figure 6** shows the effect of grain size on the consistency of the present EPO hemostat, as a function of the amount of water. The overall trend showed that the consistency of EPO hemostat increased from 14.5 to 18.5 mm with increasing amount of water, and that no marked difference in consistency was found, independent of the grain sizes of EPO, i.e., (i) 0.5–1.0 mm, (ii) 1.0–2.0 mm and (iii)  $>2.0$  mm. The present results indicate that no marked difference in such physical and chemical properties of EPO appears to exist, independent of the difference in grain size. The relationship between the amount of water and consistency of EPO hemostats with different grain sizes may be

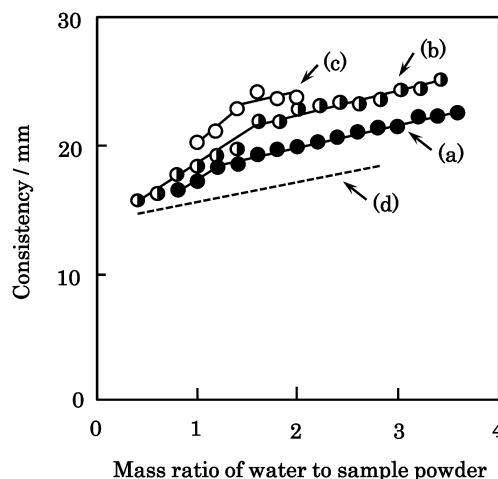


Fig. 7. Changes in consistencies of composites with POs-Ca/EPO mass ratios of (a) 0.1, (b) 0.2, (c) 0.4 and (d) pure EPO with increasing amount of water.

expressed as linear functions, e.g.,  $y = ax + b$ ,<sup>16)</sup> where  $x$  and  $y$  indicate the amount of water and consistency of the EPO hemostat, respectively. A linear regression analysis and fitting indicate  $a$ : 1.62–1.71,  $b$ : 13.80–14.66 and  $R^2$  (coefficient of determination): 0.94–0.98. On the basis of such analysis, no marked effect of grain size is found for the consistency of hemostat. In this research, we selected the EPO powder with the grain sizes of 1.0–2.0 mm for further experiments.

The changes in consistency of POs-Ca/EPO composite hemostat containing various amounts of POs-Ca were further measured by changing POs-Ca/EPO ratio and amount of water. The results are shown in **Fig. 7**. The overall trend showed that the consistency of the composite hemostat increased with increasing POs-Ca/EPO ratio and amount of water addition. Taking notice of the water content, the steady-state increase in consistency was found after the rapid increase in consistency at the initial stage of water addition.

The addition of POs-Ca contributes to enhancing the consistency of composite hemostat. This phenomenon is explained by assuming that the high dissolution of POs-Ca in water may enhance the fluidability of EPO, thereby showing the higher consistency. On further increase in the amount of water, the slopes of the linear relationship between amount of water and consistency of POs-Ca/EPO hemostat are in accordance with the case of pure EPO hemostat. The linear regression analysis and fitting indicate  $a$ : 1.62–1.77,  $b$ : 13.91–18.80 and  $R^2$  (coefficient of determination): 0.9353–0.9873. The present data agree well with those of EPO hemostat, and the consistencies of POs-Ca/EPO composite hemostats in the parts of straight lines are found to be dependent upon the consistency of EPO.

We considered that the optimum POs-Ca/EPO ratio for the consistency control is 0.2, because the consistency of POs-Ca/EPO composite hemostat may be controlled over the wider range of water to powder ratio (i.e., 0.5 to 4.0). The changes in consistencies of EPO, POs-Ca/EPO composite and *s*-HAp/EPO composite hemostats with the amount of water are shown in **Fig. 8**. The overall trend showed that the consistency of POs-Ca/EPO composite hemostat increased with increasing amount of water, but that the consistency of *s*-HAp/EPO composite hemostat remained unchanged, regardless of the increase in amount of *s*-HAp.

The linear regression analysis and fitting to the case of POs-

Ca/EPO composite hemostat indicate  $a = 1.70x + 18.8$ , whereas those of *s*-HAp/POs-Ca show  $a = 0.43x + 15.0$ . The significant increase in consistency was found for the case of POs-Ca/EPO composite hemostat, compared to the case of *s*-HAp. As already mentioned, the fluidability of EPO seems to be enhanced by the dissolution of POs-Ca in water, thereby enhancing the consistency.

### 3.3 Properties of composite hemostats

Since the POs-Ca/EPO and *s*-HAp/EPO composite hemostats could be prepared under the optimized conditions, the properties of resulting hemostats were examined in this section. The stanching times of the composites were:  $6.0 \pm 0.5$  h (*s*-HAp/EPO)  $\gtrsim 5.75 \pm 0.25$  h (POs-Ca/EPO)  $> 4.75 \pm 0.25$  h (pure EPO). The time for surgery operation is estimated to be 2 to 3 h, indicating that the time for stanching the blood may be satisfactory for the utilization as a hemostat. Since the POs-Ca and EPO are water soluble, the stanching performances of the EPO and POs-Ca/EPO composite hemostats seem to be reduced

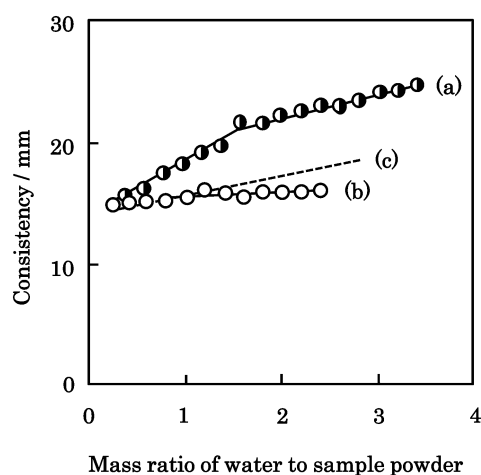


Fig. 8. Changes in consistencies of (a) POs-Ca/EPO composite hemostat with the mass ratios of 0.2, (b) *s*-HAp/EPO composite hemostat with the mass ratio of 0.2 and (c) pure EPO with increasing amount of water.

by the instantaneous penetration of simulated blood in the space formed with the dissolution of POs-Ca and EPO.

These hemostats were implanted in the femur and tibia of the Japanese white rabbit. The microscopic examination of the specimens in the femur and tibia of the Japanese white rabbit was conducted using the sectioned specimen (Villanueva bone stain). The photographs and optical micrographs of sectioned specimens after the implantation of them in the periods of 4 and 9 weeks are shown in Fig. 9. The results on the implantation for 4 weeks showed that the significant bone regeneration, together with the formation of osteoid (see the arrow marks), was found for the case of *s*-HAp/EPO composite and EPO hemostats, compared to the case of POs-Ca/EPO composite hemostat. On further increase in implantation period to 9 weeks, the bone regeneration was significant for the POs-Ca/EPO composite hemostat within the femur and tibia, as well as the case of *s*-HAp/EPO composite and EPO hemostats.

For the sample with the implantation for 4 weeks, the retarded bone regeneration for the case of POs-Ca/EPO composite hemostat may be attributed to the rapid dissolution of POs-Ca at the initial stage of implantation. Nevertheless, the significant bone regeneration is found for the case of POs-Ca/EPO composite hemostat after the implantation for 9 weeks. As is the case of implantation for 4 weeks, the excellent bone regeneration is found for the *s*-HAp/EPO composite and EPO hemostats, in contrast to the case that parts of the original hemostat remained when the commercial bone wax was implanted into the femur and tibia of Japanese white rabbits for 9 weeks (not shown here).

Further, we incorporated gentamicin, a typical antibiotic, into these hemostats, and examined the releasing behavior of it into the PBS(−). The releasing behaviors of gentamicin from the composites in the PBS(−) are shown in Fig. 10. The overall trend reveals that gentamicin was released with increasing immersion time to 10 h. The amounts of gentamicin were classified as follows: POs-Ca/EPO hemostat ( $424.1 \text{ mg} \cdot \text{cm}^{-3}$ )  $>$  EPO hemostat ( $230.6 \text{ mg} \cdot \text{cm}^{-3}$ )  $>$  *s*-HAp/EPO hemostat ( $172.0 \text{ mg} \cdot \text{cm}^{-3}$ ). It should be noted that the steady state of gentamicin releasing was found in the case of *s*-HAp/EPO hemostat. This fact suggests that the amount of gentamicin released from the EPO may be controlled by using the *s*-HAp. In this case, HAp

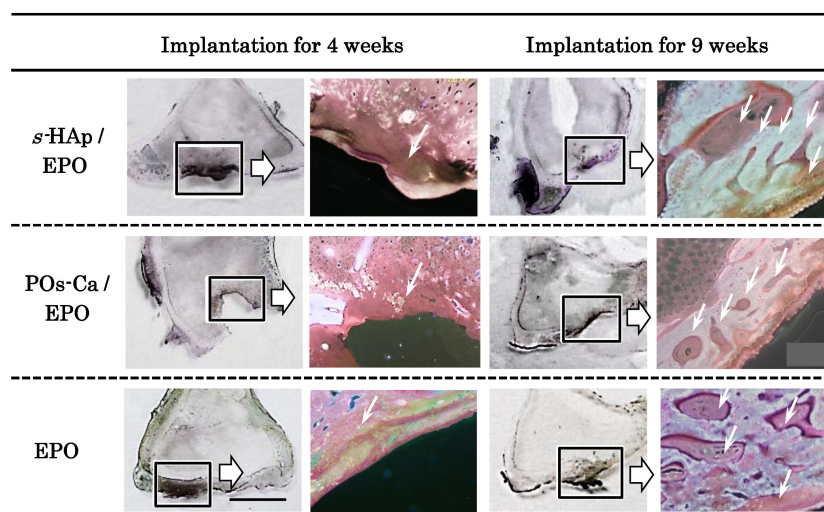


Fig. 9. (Color online) Photographs (overall views) and optical micrographs (Villanueva bone stain) of sectioned specimens of EPO, POs-Ca/EPO composite and *s*-HAp/EPO composite hemostats implanted in the femur and tibia of Japanese white rabbits. Note that the arrows in the micrographs indicate the typical formation of osteoid. A bar in EPO photograph indicates the size of 5 mm.



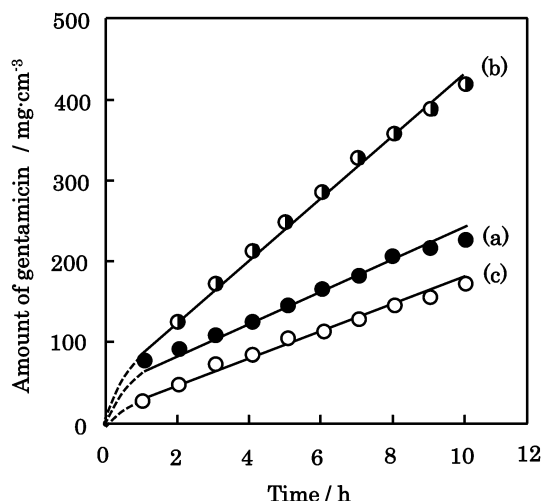


Fig. 10. Changes in amount of gentamicin in PBS(–) solution from (a) EPO, (b) POs-Ca/EPO composite hemostat with the mass ratios of 0.2 and (c) s-HAp/EPO composite hemostat with the mass ratio of 0.2 with increasing immersion time.

particles within s-HAp may contribute to adsorbing gentamicin, thereby retarding the release of it in PBS(–).

In order to quantitatively check the drug releasing behavior, the data were fitted to typical kinetic equations, i.e., (i) zero-order equation ( $Q_t = Q_0 + k_0t$ ), (ii) first-order equation ( $\ln Q_t = \ln Q_0 - k_1t$ ) and (iii) Higuchi's equation ( $Q_t = k_2t^{1/2}$ ).<sup>17)</sup> Here  $Q_0$  and  $Q$  are the amounts of release at time = 0 and  $t$ , respectively, while  $k_0$ ,  $k_1$  and  $k_2$  indicate the release rates. Among these equations, the zero-order equation seems to show the best fitting for describing the releasing behavior of gentamicin as proved by the level of coefficient of determination ( $R^2$ ) which gave higher values ranging from 0.9885 to 0.9945, compared to the case of first-order equation ( $R^2$ : 0.9087 to 0.9908) and Higuchi's equation ( $R^2$ : 0.9091 to 0.9854). The equations fitted to zero-order equation are:  $Q_t = 18.35t + 55.00$  for EPO hemostat,  $Q_t = 38.114t + 53.137$  for POs-Ca/EPO composite hemostat, and  $Q_t = 17.75t + 30.87$  for s-HAp/EPO composite hemostat. The hemostat containing s-HAp and EPO is effective for the steady state releasing of gentamicin sulfate over the longer period.

#### 4. Conclusion

Novel hemostatic agent was prepared using hydroxyapatite [ $\text{Ca}_{10}(\text{PO}_4)_6(\text{OH})_2$ ; HAp], thermoplastic resin (EPO) and POs-Ca. The drug releasing behavior of gentamicin in the PBS(–) saline solution from the EPO was examined using the hemostat. The results obtained were summarized as follows:

- (1) The starting EPO gel was obtained by the flash freezing at  $-80^\circ\text{C}$  and then freeze-drying at  $-50^\circ\text{C}$  for 15 h.

The freeze-dried materials were sieved in order to obtain the EPO powder with sizes of 1 to 2 mm. The non-stoichiometric HAp particles with the Ca/P ratio of 1.56, which had been prepared by hydrothermally heating the POs-Ca at  $100^\circ\text{C}$  for 5 h, were further mixed with EPO powder. Then the de-ionized water was put into the mixed powder to form the EPO gels with HAp in order to form the composite.

- (2) The test for the implantation of s-HAp/EPO hemostat into the Japanese white rabbits showed the excellent bone regeneration, compared to the case of POs-Ca/EPO composite hemostat. Moreover, the hemostat containing s-HAp and EPO (s-HAp/EPO = 0.20) was effective for the steady state releasing of gentamicin sulfate, as well as the inhibition of bleeding.

**Acknowledgements** The authors are expressed their thanks to Oji Cornstarch Co., Ltd. for providing POs-Ca powder.

#### References

- 1) S. Samudrala, *AORN J.*, **88**, S2–S18 (2008).
- 2) A. Harjula, *Scand. J. Thorac. Card. Surg.*, **17**, 277–281 (1983).
- 3) T. Wellisz, J. K. Armstrong, J. Cambridge and T. C. Fisher, *J. Craniofacial Surg.*, **17**, 420–425 (2006).
- 4) A. V. Kabanov, E. V. Batrakova and V. Y. Alakhov, *J. Controlled Release*, **82**, 189–212 (2002).
- 5) H. Kamasaka, K. To-o, K. Kusaka, T. Kuriki, T. Kometani, H. Hayashi and S. Okada, *Biosci. Biotechnol. Biochem.*, **61**, 238–244 (1997).
- 6) H. Kamasaka, D. Inaba, K. Minami, T. Nishimura, T. Kuriki and M. Yonemitsu, *Trends Glycosci. Glycotechnol.*, **15**, 75–89 (2003).
- 7) T. Umeda, K. Itatani, H. Mochizuki, I. J. Davies, Y. Musha and S. Koda, *Key Eng. Mater.*, **309–311**, 515–518 (2006).
- 8) C. Hama, T. Umeda, Y. Musha, S. Koda and K. Itatani, *J. Ceram. Soc. Japan*, **118**, 446–450 (2010).
- 9) S. Kumagai and K. Itatani, *Phosphorus Res. Bull.*, **25**, 078–086 (2011).
- 10) J. Guicheux, G. Grimandi, M. Trecant, A. Faiver, S. Takahashi and G. Daculsi, *J. Biomed. Mater. Res.*, **34**, 165–170 (1997).
- 11) M. Itokazu, W. Yang, T. Aoki and N. Kato, *Biomaterials*, **19**, 817–819 (1998).
- 12) Joint Committee on Powder Diffraction Standards, The International Centre for Diffraction Data No. 09-0432, Newton Square, PA, USA (1959).
- 13) Y. Arai and T. Yasue, *Gypsum & Lime.*, **188**, 52–55 (1984).
- 14) J. P. Lafon, E. Champion and D. Bernache-Assollant, *J. Eur. Ceram. Soc.*, **28**, 139–147 (2008).
- 15) Joint Committee on Powder Diffraction Standards, The International Centre for Diffraction Data No. 55-0898, Newton Square, PA, USA (2005).
- 16) M. Kumar, N. P. Singh and N. B. Singh, *Indian J. Chem. Technol.*, **16**, 499–506 (2009).
- 17) S. Dash, P. N. Murthy, L. Nath and P. Chowdhury, *Acta Polon. Pharm. Drug Res.*, **67**, 217–223 (2010).